Human L-ferritin deficiency is characterized by idiopathic generalized seizures and atypical restless leg syndrome

Anna Cozzi,[1] Paolo Santambrogio,[1] Daniela Privitera,[2] Vania Broccoli,[1] Luisa Ida Rotundo,[1] Barbara Garavaglia,[3] Rudolf Benz,[4] Sandro Altamura,[5] Jeroen S. Goede,[6] Martina U. Muckenthaler,[5] and Sonia Levi[1,2]

[1]San Raffaele Scientific Institute, Division of Neuroscience and [2]University Vita-Salute San Raffaele, 20132 Milano, Italy
[3]Molecular Neurogenetics Unit, Istituto Di Ricovero e Cura a Carattere Scientifico Foundation Neurological Institute "Carlo Besta," 20126 Milano, Italy
[4]Department of Internal Medicine, Kantonsspital Münsterlingen, 8596 Münsterlingen, Switzerland
[5]Department of Pediatric Oncology, Hematology and Immunology, Molecular Medicine Partnership Unit, University of Heidelberg, 69120 Heidelberg, Germany
[6]Division of Hematology, University Hospital, 8091 Zurich, Switzerland

The ubiquitously expressed iron storage protein ferritin plays a central role in maintaining cellular iron homeostasis. Cytosolic ferritins are composed of heavy (H) and light (L) subunits that co-assemble into a hollow spherical shell with an internal cavity where iron is stored. The ferroxidase activity of the ferritin H chain is critical to store iron in its Fe3+ oxidation state, while the L chain shows iron nucleation properties. We describe a unique case of a 23-yr-old female patient affected by a homozygous loss of function mutation in the L-ferritin gene, idiopathic generalized seizures, and atypical restless leg syndrome (RLS). We show that L chain ferritin is undetectable in primary fibroblasts from the patient, and thus ferritin consists only of H chains. Increased iron incorporation into the FtH homopolymer leads to reduced cellular iron availability, diminished levels of cytosolic catalase, SOD1 protein levels, enhanced ROS production and higher levels of oxidized proteins. Importantly, key phenotypic features observed in fibroblasts are also mirrored in reprogrammed neurons from the patient's fibroblasts. Our results demonstrate for the first time the pathophysiological consequences of L-ferritin deficiency in a human and help to define the concept for a new disease entity hallmarked by idiopathic generalized seizure and atypical RLS.

Alterations in brain iron homeostasis are a hallmark of neurodegenerative diseases (Berg and Youdim, 2006). Localized iron overload is associated with both Alzheimer's and Parkinson's disease (Altamura and Muckenthaler, 2009), and with a group of genetic disorders termed neurodegeneration with brain iron accumulation (Hayflick, 2006). Besides, brain iron deficiency is related to neurodegenerative processes like restless leg syndrome (RLS; Salas et al., 2010) and epilepsy (Ozaydin et al., 2012). Several studies analyzed cerebral spinal fluid or brain samples for iron content and iron-containing proteins or by brain imaging (Clardy et al., 2006; Connor et al., 2011; Allen et al., 2001; Allen, 2004) and showed that RLS is hallmarked by

low cerebral iron levels that particularly affect the dopamine-producing cells of the substantia nigra (Connor et al., 2011). In contrast, the direct link between iron deficiency and epilepsy still remains controversial (Idro et al., 2010; Sherjil et al., 2010).

The iron storage protein ferritin plays a central role in maintaining systemic and cellular iron levels. It sequesters the metal inside of its internal cavity to satisfy cellular iron demands and to prevent toxicities arising from Fenton-like reactions (Arosio and Levi, 2010). In vertebrates, three different genes (*FTL*, *FTH*, and *FTMT*) code for ferritin proteins with a highly

The Rockefeller University Press $30.00
J. Exp. Med. 2013 Vol. 210 No. 9   1779-1791
www.jem.org/cgi/doi/10.1084/jem.20130315

1779

The Journal of Experimental Medicine

conserved 3D structure (Lawson et al., 1991; Langlois d'Estaintot et al., 2004; Luscieti et al., 2010). *FTL* and *FTH* code for cyto-solic ferritins (Arosio and Levi, 2010) that co-assemble into a heteropolymer to form a hollow spherical shell with an inter-nal cavity where iron is stored (Zhao et al., 2003). Different tissues express different ratios of the H- and L-ferritin sub-units (FtH and FtL; Arosio and Levi, 2010). The *FTMT* gene codes for a mitochondrial-targeted ferritin, which assembles into a homopolymer of 24 identical subunits (Levi et al., 2001). Both, the H and Mt ferritin subunits exert ferroxidase activity (Levi et al., 1988; Levi and Arosio, 2004), whereas the L sub-unit shows an active nucleation center on the cavity surface, which favors iron storage (Levi et al., 1992; Levi et al., 1994).

Expression of the *FTH* and *FTL* genes is regulated in re-sponse to the intracellular labile iron pool (LIP) by iron regu-latory proteins 1 and 2 (IRPs; Hentze et al., 2010). IRPs bind the iron responsive element (IRE), a RNA stem loop struc-ture located within the 5′ untranslated region of FtL and FtH mRNAs. The IRP–IRE complex is formed under iron-deficient conditions and prevents mRNA translation (Recalcati et al., 2010).

The critical importance of cytosolic ferritin in maintain-ing iron homeostasis is highlighted by the genetic ablation of the ferritin genes in animal models (Ferreira et al., 2000, 2001; Thompson et al., 2003; Missirlis et al., 2007; Darshan et al., 2009). In *Drosophila melanogaster* both FtH and FtL are essen-tial for embryonic development (Missirlis et al., 2007). Simi-larly, homozygous null mice for FtH die in utero, indicating that the ferroxidase activity of the H subunit is essential dur-ing mammalian embryonic development (Ferreira et al., 2000). Heterozygous ferritin-H +/− mice show mild iron deficiency (Ferreira et al., 2001) and increased indices of oxidative stress in brain tissues (Thompson et al., 2003). Conditional knock-out of the *FTH* gene in the liver induced hepatic damage and rapid cell death in mouse embryonic fibroblasts (Darshan et al., 2009).

In contrast, a deletion of the *FTL* gene in vertebrates has not been described. However, several pathogenic human mu-tations were reported in the *FTL* gene (Levi et al., 2005). These cause at least two types of dominant disorders: heredi-tary hyperferritinemia with cataract (HHCS; OMIM 600886; Beaumont et al., 1995) or (neuro)ferritinopathy (OMIM 606159; Curtis et al., 2001; Vidal et al., 2004), depending on the loca-tion of the mutation within the *FTL* gene. In subjects af-fected by HHCS, mutations most commonly occur within the IRE stem loop of the FtL mRNA (Millonig et al., 2010). These mutations reduce the affinity for IRP binding and, as a result, these patients produce 2–10 fold more FtL in tissues and serum with no associated abnormalities in iron homeostasis (Millonig et al., 2010). Excess ferritin aggregates in micro crys-tals in the lens induce nuclear and bilateral cataract (Brooks et al., 2002). Neuroferritinopathy, a rare neurodegenerative disease with autosomal and dominant transmission (Curtis et al., 2001), is caused by single or multiple nucleotides inser-tions in exon 4 of the *FTL* gene. These mutations cause frame-shifts and large alterations of the C-terminal sequence of the FtL peptide (Levi et al., 2005; Cozzi et al., 2010). The affected patients show movement disorders and abundant spherical inclusions that contain ferritin and iron in the brain and other organs (Burn and Chinnery, 2006). Furthermore, patients carrying the heterozygous missense mutation Thr30Ile and the recently identified Gln26Ile and Ala27Val show hyperfer-ritinemia and an increased amount of glycosylated ferritin (Kannengiesser et al., 2009; Thurlow et al., 2012), whereas haploinsufficiency occurs in a subject with an altered start codon in one allele, which caused abnormally low levels of FtL in serum and tissues (Cremonesi et al., 2004).

Here, we describe the first patient with a complete loss of FtL function caused by a homozygous mutation (310G>T), located in exon 3 of the FtL gene, which generates a stop codon at aa 104. The patient was affected by idiopathic gen-eralized seizures during infancy and atypical RLS, as defined by polysomnography in the absence of periodic limb move-ments. Molecular analyses reveal that the truncated peptide is unable to assemble with the H subunit to form the full ferri-tin cage. Fibroblasts derived from the patient that exclusively express a H chain homopolymer are hallmarked by alterations of cellular iron homeostasis and oxidative stress; findings mir-rored in induced neurons (iNs) from the patient.

RESULTS

Detection of a homozygous STOP codon at amino acid 104 of the *FTL* gene in a patient

In our patient with undetectable serum ferritin levels, idio-pathic generalized seizures, and atypical RLS, we screened all exons encoding the FTL gene for neuroferritinopathy-associated mutations and detected a G>T nucleotide substi-tution (G310T) in exon 3 (Fig. 1 A). This base substitution generates a stop codon in the corresponding amino acid 104 (E104X; Fig. 1 B, top). The 3D structure of ferritin containing L subunits (Ford et al., 1984) predicts that amino acid residue E104 is located in the middle of α-helix C (Fig. 1 B, bottom), where it engages a salt bridge with aa K58. This salt bridge was described to be critical for the stability of the full molecule (Santambrogio et al., 1992). Mutational studies on ferritin peptides (Levi et al., 1989, 1994; Yewdall et al., 1990; Luscieti et al., 2010) suggest that a stop codon at this position produces a truncated peptide unable to fold into a full ferritin cage.

FtL expression is not detectable in fibroblasts from a patient with the FtL G 310>T variant

To analyze the expression of the FtL variant in our patient, we derived fibroblasts (termed E104X) from a patient's skin bi-opsy and from three healthy control subjects (termed CTR1, CTR2, and CTR3). To determine ferritin subunit compo-sition in E104X and control fibroblasts, we metabolically labeled the cells with 50 μCi [^{35}S]methionine for 18 h and prepared cellular homogenates that were sequentially immu-noprecipitated, first with anti–ferritin L chain (αFtL) and then with anti–H chain (αFtH) antibodies (Fig. 1 C). Although FtL was detectable in control fibroblasts, the predicted ∼11-kD L chain variant could not be detected in E104X cells. In addition,
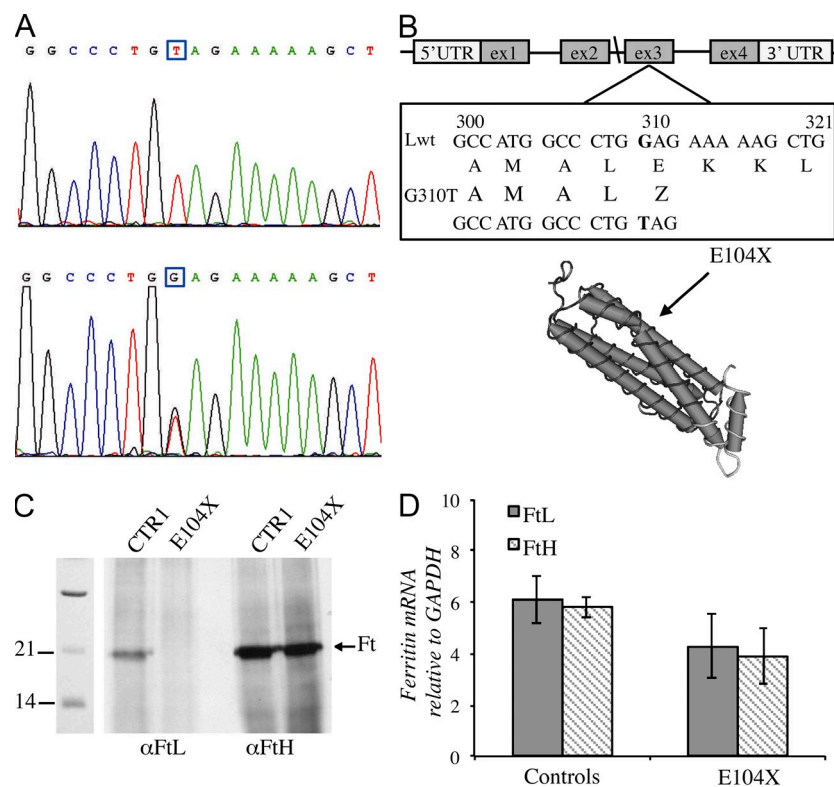
Figure 1. FtL expression is undetectable in fibroblasts from a patient with the FtL G 310>T variant. (A, top) The pherogram shows the homozygous G>T exchange at nt 310 (counted from the first nucleotide of the starting codon) in exon 3 of the patient's ferritin gene and (bottom) the corresponding heterozygous mutation in parent's DNA is shown. (B) Sequence alignment of the partial exon 3 of the human FtL (Lwt) and FtL variant (G310T), as well as the 3D structure scheme of L ferritin subunits. The arrow indicates the mutated position. (C) [35S]methionine–labeled ferritin. Fibroblasts derived from the patient (E104X) and a control proband (CTR1) were metabolically labeled with 50 µCi/ml [35S]methionine for 18 h and lysed, and then 4 × 10⁶ cpm of the homogenates were precipitated with saturating amounts of anti–FtL antibody (αFtL). The soluble fraction was precipitated again with an anti-FtH antibody (αFtH) and analyzed on a 12% SDS-PAGE, which was subjected to autoradiography. One of two representative experiments. (D) Ferritin mRNA levels were determined by quantitative real-time PCR for FtL and FtH and normalized to mRNA expression of GAPDH. Data are the mean ± SD values of three independent experiments.

FtL was not detectable in E104X fibroblasts by application of a specific ELISA, whereas FtH levels were comparable in all control cells (Table 1), suggesting a similar capacity for iron incorporation. Importantly, the amount of FtL mRNA expression was similar in E104X and control cells, and FtH

chain expression was not impaired by the lack of L chain expression in E104X fibroblasts (Fig.1 D).
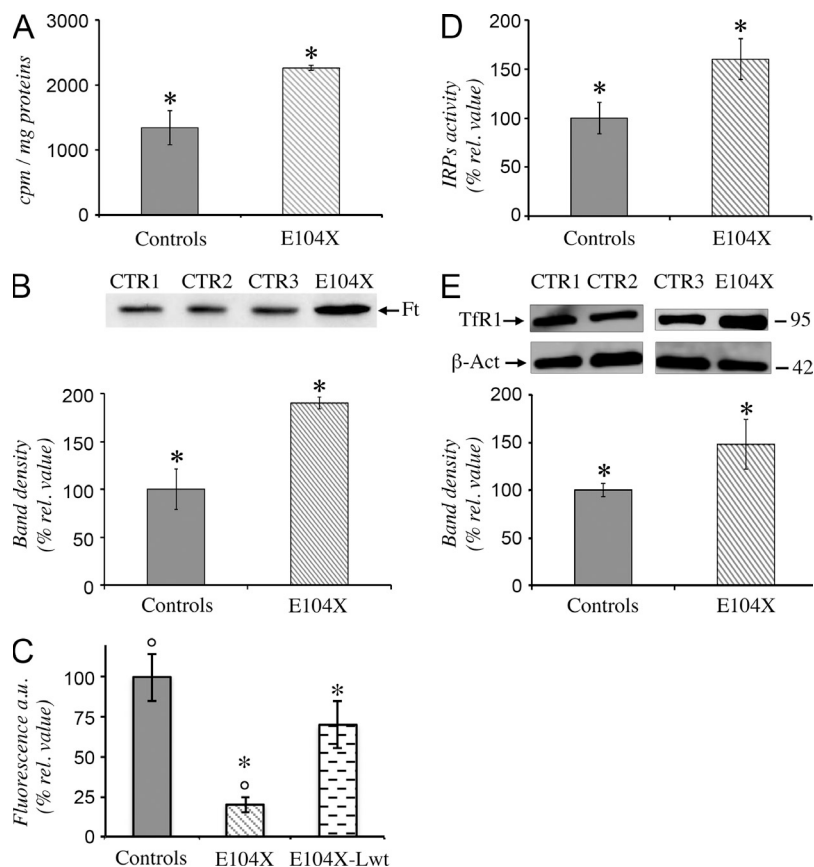
H homopolymer ferritin formation induces iron deficiency
To analyze ferritin properties in E104X fibroblasts, we treated cells with 2 µCi 55Fe-ammonium citrate (FAC) for 18 h. Total cellular 55Fe levels (Fig. 2 A) and incorporation of iron into ferritin (Fig. 2 B) were increased by approximately twofold in E104X fibroblasts compared with control cells, as detected by counting radiolabeled iron and by autoradiography of cellular extract electrophoretic analysis, respectively. Increased iron incorporation into ferritin may cause intracellular iron starvation that can be monitored by the level of the LIP. Thus, we next analyzed the LIP by a fluorescent-permeable metal sensor, calcein-AM (Picard et al., 1998). Fibroblasts were incubated with 0.250 µM calcein–AM for 15 min at 37°C, and an increase in fluorescence emission at 535 nm was monitored after addition of the permeable chelator deferiprone (Fig. 2 C). The basal LIP level of E104X cells was approximately fourfold lower compared with the controls. To verify if the absence of L chain expression was the cause for the LIP reduction, we

Table 1. Ferritin level

	FtL (ng/mg prot.)	FtH (ng/mg prot.)
CTR1	11 ± 1.5	162 ± 12.7
CTR2	19 ± 7.0	116 ± 17.0
CTR3	10 ± 3.0	133 ± 23.0
E104X	Undetected	148 ± 23.0
E104X-Lwt	14 ± 1.0	135 ± 33.0

L (FtL) and H (FtH) chain ferritin was analyzed in cell extracts of fibroblasts from three different healthy control probands, our patient (E104X), and patient fibroblasts with forced FtL expression (E104X-Lwt) by an ELISA. The results are shown as nanograms/milligram of ferritin of total soluble proteins. The values are the means and SD of three independent experiments.

Figure 2.   H homopolymer ferritin formation induces iron deficiency. Iron incorporation into cells and ferritin was analyzed in 2×10^5 cells incubated for 18 h in medium supplemented with 2 µCi/ml ^{55}Fe-FAC. (A) Cellular ^{55}Fe incorporation. Radioactivity of total soluble homogenates expressed as cpm/mg of total proteins. *, $P \leq 0.001$. (B) Ferritin ^{55}Fe incorporation. Samples of soluble cell homogenates containing 10 µg of protein were separated on a 7% nondenaturing PAGE (the arrow indicates ferritin mobility), exposed to autoradiography, and evaluated by densitometry. The results are expressed as relative value to the mean of the controls of three independent experiments. *, $P \leq 0.001$. (C) LIP. The assay was performed with 4×10^4 cells; they were incubated with 0.250 µM calcein-AM for 15 min at 37°C, and then with cells. The increase in fluorescence emission at 535 nm was monitored after addition of the permeable iron chelator deferiprone (0.2 mM). °, $P \leq 0.002$; *, $P \leq 0.001$. (D) IRP activity. 2 µg of total soluble protein extracts were incubated with a ^{32}P-labeled IRE-ferritin probe in the absence or presence of 2% 2-mercaptoethanol, and RNA–protein complexes were separated on 6% nondenaturing PAGE and exposed to autoradiography. Mobility shifted bands were quantified. *, $P \leq 0.05$. (E) TfR1 expression. 20 µg of soluble cell homogenates were separated on a 12% SDS-PAGE, blotted, and incubated with an anti–human TfR1 antibody. Quantification was performed by densitometry. *, $P \leq 0.05$. Results in C–E show the mean of three independent experiments.

overexpressed the wild-type L chain ferritin in E104X fibroblasts (named E104X-Lwt) by transduction with a lentiviral vector (Lv-GFP-FtL; Cozzi et al., 2010). Transduction efficiency was visualized by monitoring GFP cells and was shown to be up to 60%. 10 d later, the expression of FtH and FtL was assayed by ELISA (Table 1). As expected, ferritin levels were now similar to that of the controls, and the LIP recovered up to ~75% of the controls (Fig. 2 C). To further assay cellular iron availability, we analyzed the IRP binding activity by electrophoretic mobility shift assay (EMSA) and transferrin receptor 1 (TfR1) expression by immunoblotting. Consistent with reduced iron availability in E104X fibroblasts, both IRP binding activity (Fig. 2 D) and TfR1 expression (Fig. 2 E) were increased by ~1.5-fold compared with control cells. Collectively, these data suggest that a lack of FtL results in an increased iron binding capacity of the FtH homopolymer and

reduced cellular iron availability, which can be compensated for by forced FtL expression.

H homopolymer ferritin formation triggers oxidative stress and cellular damage
Free iron promotes the formation of free radicals, and thus we hypothesized that reduced iron levels detected in fibroblasts may improve resistance to oxidative stress. To test this, the viability of fibroblasts was analyzed by the MTT assay after treatment with 0.6 mM H_2O_2 for 2 h. Unexpectedly, the oxidative insult decreased the number of viable E104X fibroblasts by ~25% compared with 10% in control cells (Fig. 3 A). To further investigate the increased sensitivity to oxidative insult, fibroblasts were incubated with increasing concentrations of H_2O_2 for 30 min and ROS levels were determined by dihydrorhodamine 123 (DHR-123). Interestingly, we observe a
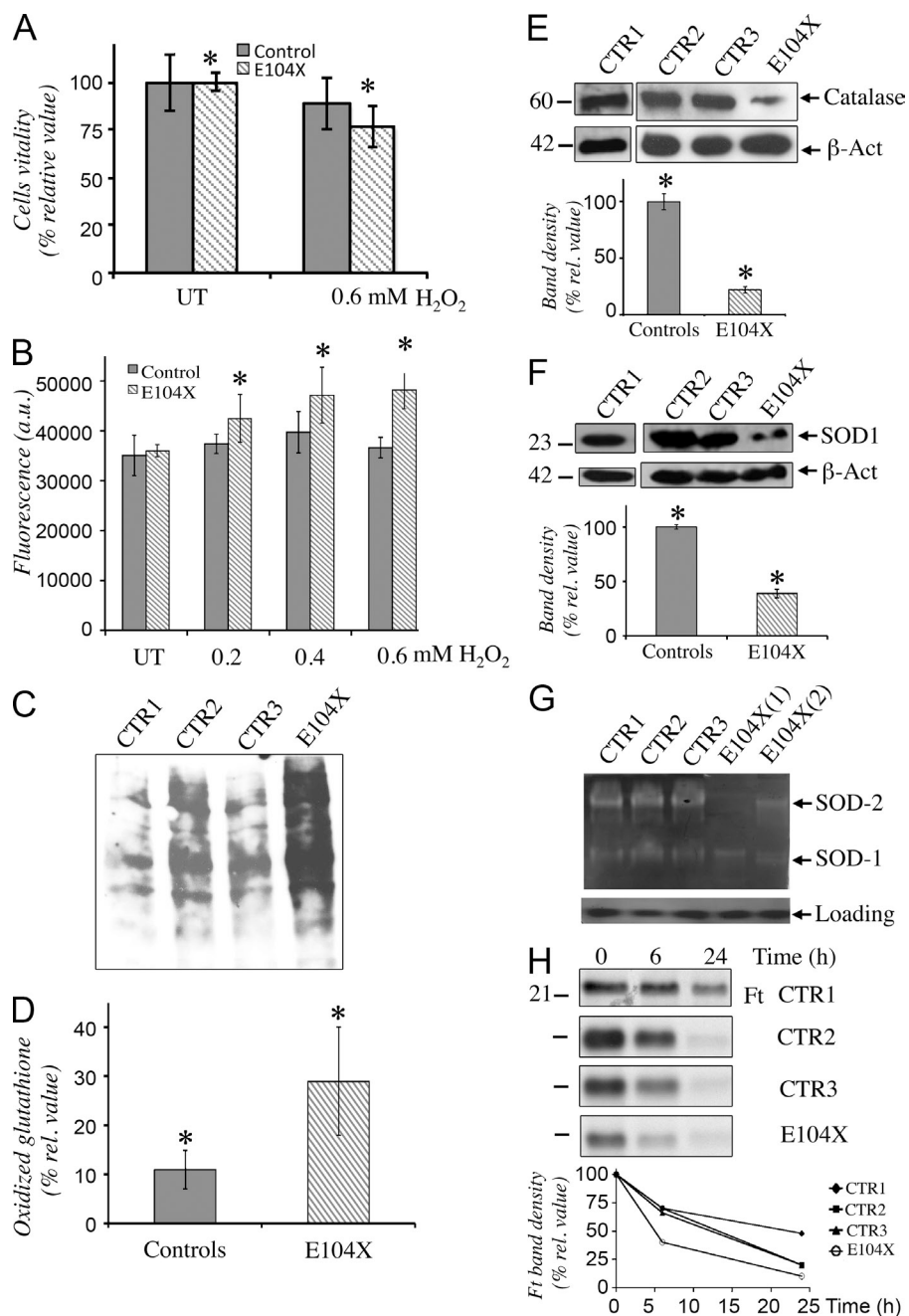
Figure 3. **H homopolymer ferritin induces oxidative damage and shows a reduced half-life.** (A) Cellular vitality. Cells (10^4) were incubated for 2 h with 0.6 mM H_2O_2 in serum-free medium and cellular vitality was measured by MTT assay. Data are the mean of two independent experiments in octoplicate. *, P ≤ 0.05. (B) ROS levels. Cells (10^4) were incubated for 15 min with 30 µM of dihydrorhodamine, washed, and treated with different amounts of H_2O_2 for 30 min. Fluorescence was measured at 535 nm. Results are the mean of two independent experiments in octoplicate. *, P ≤ 0.05. (C) Oxidized proteins. The levels of carbonylated proteins were analyzed by oxyblot (see Materials and methods). (D) GSSG. 10^4 cells were treated or not with 5 mM of TCEP (tris(2-carboxyethyl)phosphine) for 20 min at room temperature and analyzed according to the manufacturer's instructions. Oxidized glutathione is shown as relative value of the total. Shown is a representative experiment, in triplicate, of two independent experiments. *, P ≤ 0.009. Catalase and SOD1 expression. 25 µg of total soluble proteins were separated on a 12% SDS-PAGE, blotted, and incubated with an anti-catalase (E) or anti-SOD1 (F) antibodies. Quantification of bands was performed by densitometry. The results show the mean of three experiments. *, P ≤ 0.001. (G) SOD activities. Fibroblast cell extracts (15 µg) of controls (CTR) and patient (E104X) were loaded on a 12% nondenaturing PAGE and analyzed for SOD activities by nitroblue tetrazolium staining. SOD2 and SOD1 indicate the activity of the mitochondrial MnSOD2 and cytosolic SOD1 enzymes, respectively. The two extracts E104X (1) and (2) indicate the extreme points of the variability range. One representative of four independent experiments is shown. (H) Ferritin turnover. L-variant and control cells were metabolically labeled for 18 h with 50 µCi/ml ^{35}S-methionine in methionine-free medium. After washing, the cells were maintained in complete medium for the indicate times. (top) 10 µg of soluble proteins were immunoprecipitated with saturating amounts of anti–ferritin-H (αFtH). The precipitated proteins were separated on a 12% SDS-PAGE. The gels were exposed to autoradiography. The arrows indicate the ferritin subunits. One representative of two independent experiments is shown. (bottom) Densitometry quantification of ferritin is shown as percentage of the initial signal.

significant increase in ROS production in E104X fibroblasts (Fig. 3 B), whereas control fibroblasts seem to appropriately buffer the consequences of H_2O_2 addition. We further show that the levels of carbonylated proteins under basal conditions, as assessed by oxyblot, were increased in E104X cells (Fig. 3 C). To corroborate these results, we also determined glutathi-one levels in fibroblasts treated or not with 5 mM of reduc-ing agent tris(2-carboxyethyl)phosphine (TCEP) for 20 min (Schulz et al., 2000). Consistent with an increased oxidative status in E104X fibroblasts, an approximately twofold increase in the oxidized form of glutathione (GSSG) was observed compared with the mean of control cells (Fig. 3 D). More-over, immunoblotting of ROS scavenger proteins shows a reduction of catalase (Fig. 3 E) and superoxide dismutase1 (SOD1; Fig. 3 F) by ~75 and 60%, respectively, in E104X cells compared with control subjects. In addition, SOD1 and SOD2 activities are reduced (Fig. 3 G), despite unchanged SOD2 protein levels (not depicted). In contrast, mRNA ex-pression for all the three scavenger proteins analyzed is unal-tered (unpublished data).

H homopolymer ferritin shows a reduced half-life

Both increased oxidative stress (Mehlhase et al., 2005) and iron deficiency (De Domenico et al., 2009) promote ferritin degradation. To test whether ferritin turnover was altered in E104X fibroblasts, we investigated the ferritin degradation rate by pulse chase experiments. Cells were metabolically la-beled with 50 μCi [^{35}S]methionine for 18 h, and ferritin was immunoprecipitated at the indicated times applying an anti–H chain antibody (αFtH). In control cells, the ferritin half-life was 18 h as previously reported (Cozzi et al., 2006), whereas it was reduced to 5 h in E104X cells (Fig. 3 H).

Neurons derived from patient fibroblasts show increased ROS level without alteration of the mitochondrial membrane potential

To assess whether increased oxidative stress observed in E104X fibroblasts is also preserved in a cellular model more appropriate to the investigation of neuronal impairment, we took advantage of a recently developed technology, which al-lows us to directly convert human fibroblasts into neuronal cells (Vierbuchen and Wernig, 2011). Patient fibroblasts were transduced with a cocktail of lentiviral vectors carrying the Mash1, Nurr1, and Lmx1 transcription factors under the control of a Tet-inducible promoter (Caiazzo et al., 2011). Combined expression of these transcription factors induces the formation of dopaminergic neurons (Caiazzo et al., 2011). 21 d after transduction, the expression of neuronal markers, such as neuron-specific class III β-tubulin (TuJ1) and tyrosine hydroxylase (TH) was detected by immunostaining (Fig. 4 A). The efficiency of neuronal transformation evaluated by TuJ1 positivity was similar in controls and E104X cells ranging be-tween 5 and 10% (unpublished data). TH positivity was detected in 50% of the iNs in control and patient samples (Fig. 4 A). We next quantitatively analyzed ROS levels (Fig. 4 B) and mitochondrial functionality (Fig. 4 F) in single-derived

neurons expressing the neuronal marker N-CAM using fluorescent-specific probes and the In Cell Analyzer system. N-CAM detection allows for the identification of all types of live neurons. Fluorescence of the ROS-sensor dichlorofluor-escein (DCF) was collected only from N-CAM–positive cells (~200 cells per type), and its evaluation indicated higher ROS levels in E104X neurons compared with control cells (Fig. 4 D). Next, mitochondrial membrane potential was evaluated by quantification of tetramethyl rhodamine methyl ester (TMRM) signals on N-CAM–positive cells (Fig. 4 F). Data collected from ~150 cells per type indicated that the mitochondrial membrane potential was not affected in E104X neurons (Fig. 4 F). In addition, neurons were tested for iron deficiency by analyzing TfR1 levels. Cells were stained with anti-TfR1 and TuJ1 and the fluorescence emission in neurons was quantified by the ImageJ software (Fig. 4 C). The plot showed significantly higher TfR1 expression in E104X neurons compared with control cells (Fig. 4 E), in-dicating iron deficiency.

DISCUSSION

In this study, we have identified a new disease entity that is hallmarked by a homozygous loss of function mutation in the iron storage protein FtL, idiopathic generalized seizures, and atypical RLS. Fibroblasts and neurons derived from the fibroblasts of this patient show signs of cytosolic iron deficiency and oxidative damage, which may explain the clin-ical findings.

The mutation identified in the *FTL* gene at nucleotide position 310 (G to T) causes a homozygous stop codon. Trun-cations at this position are incompatible with the folding of a functional FtL peptide and thus lead to a loss of FtL func-tion. As a consequence, only H homopolymer ferritin type is formed in all patients' cells. Thus, for the first time, we were able to study human cells completely deficient of the FtL subunit. Up until now, human ferritin L subunit deficiency was only studied in HeLa cells after RNA interference (Cozzi et al., 2004), whereas FtL knockout mice have not been reported. Thus, we provide for the first time data on the pathophysiological consequences of FtL deficiency in an en-tire organism.

A G>T nucleotide substitution at position 310 of exon 3 results in a premature termination codon, which we expected to be recognized by mRNA quality control mechanisms and degradation by the nonsense-mediated mRNA decay ma-chinery (Isken and Maquat, 2007). However, FtL mRNA levels were similar in the patient's fibroblasts and controls (Fig. 1 D), suggesting that, similar to some mutations in the human β-globin gene (Romão et al., 2000), this stop codon may escape mRNA quality surveillance. Previous mutational studies on recombinant FtH (Levi et al., 1989; Yewdall et al., 1990; Levi et al., 1994; Luscieti et al., 2010) suggested that protein truncations (Levi et al., 1989) that occur 5′ to aa 155 in the FtH protein were unable to fold appropriately and assemble in a 24-mer shell. Because of the high structural homology of the FtH and FtL peptides, the L-variants are
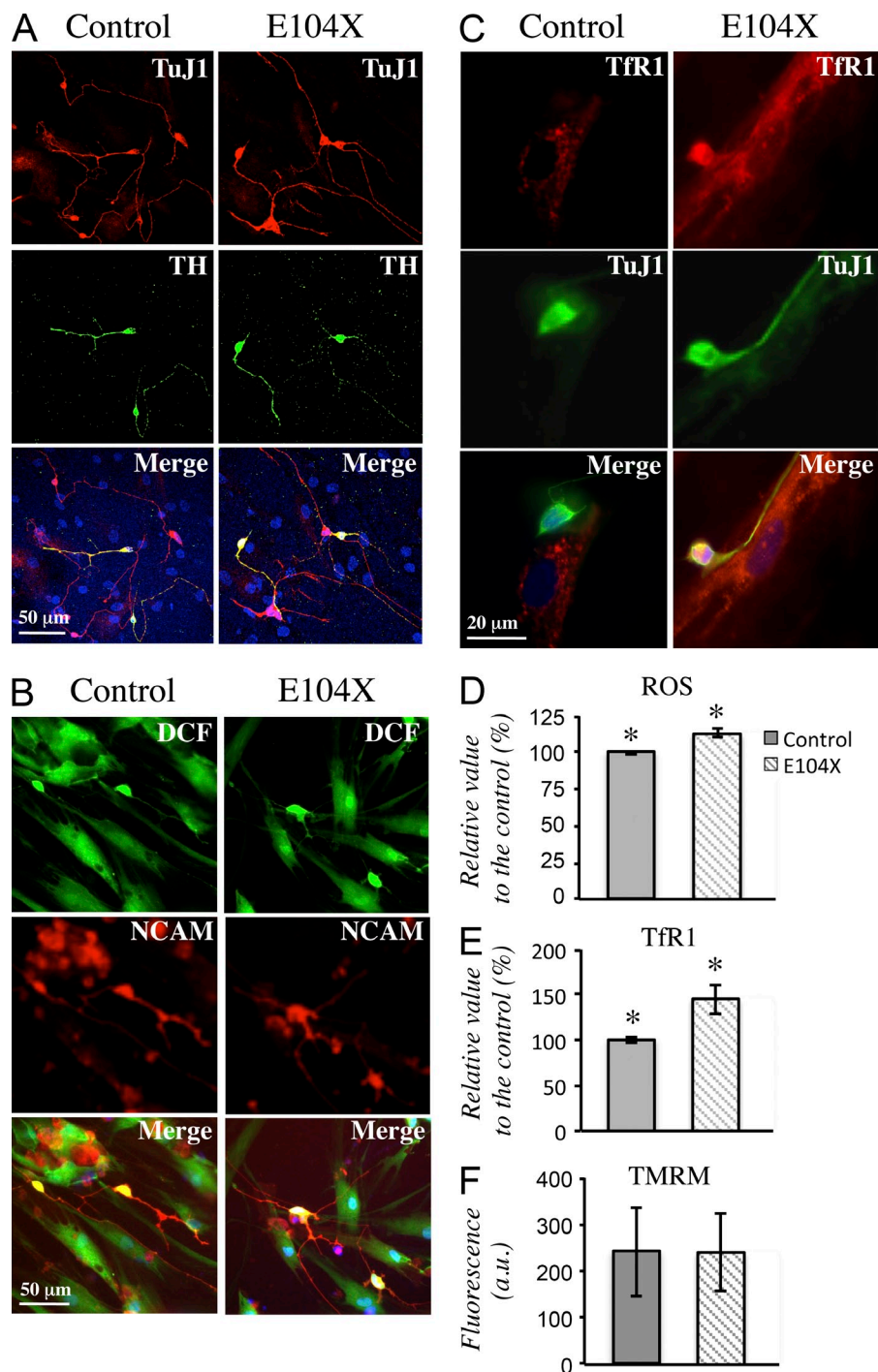
Figure 4. **iNs show increased ROS level and TfR1 expression, and unaffected mitochondrial membrane potential.** Confocal analysis of control and E104X cells (A) stained with TuJ1 (top) and TH (middle); merge (bottom). (B) Control and E104X live cells analyzed by IN-cell analyzer stained with the ROS sensible fluorescent probe DCF (top) and with the neuronal specific anti–N-CAM antibody (middle); merge in the (bottom). (C) Control and E104X fixed cells were analyzed for TfR1 signal (top) and with neuronal specific anti-TuJ1 antibody (middle); merge in the (bottom). (D) DCF fluorescence from N-CAM–positive cells (from B) were quantified, and the data are shown in the plots (mean ± SEM). *, P ≤ 0.004. Results are the mean of three independent experiments (total of ∼200 neurons for each subject). (E) TfR1-associated fluorescence from TuJ1-positive cells (from C) were quantified and the data are shown in the plots (mean ± SEM). *, P ≤ 0.007. Results are the mean of three independent experiments (total of ∼20 neurons for each subject). (F) TMRM fluorescence signal from the N-CAM–positive cells were quantified (total of ∼150 neurons for each subject), and the data are shown in the plot. Results are the mean of three independent experiments (mean ± SEM).

expected to behave in a similar manner. Indeed our qualitative and quantitative analysis of FtL expression suggests that the full ferritin protein cage lacks the FtL subunit in fibroblasts derived from the patient. Thus, the disease phenotype may result either from a loss of FtL function or a gain of function via altered activity of the FtH homopolymer. Importantly, we did not detect an increased amount of FtH expression, suggesting that a compensatory effect between the two genes does not exist, at least in the cell type studied.

The FtL functionality data, obtained by overexpression (Cozzi et al., 2000) and RNA interference studies in HeLa cells (Cozzi et al., 2004), indicated that alterations of FtL levels do not affect cellular iron homeostasis or the sensitivity to oxidative stress. The only effect detected in cells overexpressing FtL was increased cell proliferation that likely resulted from iron-independent mechanisms. RNA interference reduced FtL expression by ∼80%, suggesting that 1 or 2 FtL ferritin subunits are still incorporated in the heteropolymer.

Moreover, in vitro–reconstituted H/L heteropolymers indicated that the presence of even a small proportion (2–4 chains per shell) of FtL subunits is sufficient to confer maximum functional properties to the ferritin molecule (Santambrogio et al., 1993). The data obtained in this study analyzing cells completely deficient for FtL demonstrate that we must revise our concept of the void effect of FtL deficiency on cellular iron metabolism. We show that the absence of FtL triggers cellular iron deficiency due to the higher iron avidity of the H homopolymer compared with the ferritin heteropolymer expressed in the control cells (Fig. 2 B). This finding was further corroborated by demonstrating a decrease of the LIP and an increase of IRP activity in patient's fibroblasts. As a consequence, TfR1 levels are elevated, which will pilot more iron into the cell. However, despite this compensatory response, the LIP remains low. This finding indicates that the iron incorporation capacity of FtH overcomes the ability of the cell to replenish the LIP with iron.

Iron insufficiency was recently described as a molecular mechanism for motor neuron degeneration in IRP2-null mice (Rouault and Cooperman, 2006). Impaired control of iron metabolism by IRP2 deficiency causes cellular iron starvation induced by decreased levels of the iron importer TfR1 and the overexpression of both ferritin subunits (Jeong et al., 2011). In this case, the iron supply to mitochondria was affected with the consequent impairment of organelle functionality and motor neuron degeneration (Jeong et al., 2011). In our patient who has a FtL–null allele, only SOD2 activity appears disturbed, whereas ATP production and mitochondrial membrane potential are not affected, at least in fibroblasts and in induced neuronal cells (Fig. 4 F). We speculate that the level of iron deficiency in this patient is restricted to the cytosol and that it is not severe enough to affect the mitochondrial compartment. This difference may be explained by the lower iron requirement of fibroblasts or iNs compared with motor neurons. However, this mitochondrial functional preservation sustains the hypothesis that iron supplementation to mitochondria is a priority for cells.

Furthermore, our data indicate that the patient's fibroblasts show reduced resistance to H_2O_2 treatment associated with increased ROS production compared with control cells. Indeed, the oxidative status in patient's cells is altered also under basal conditions, as indicated by the increased amount of carbonylated protein and oxidized glutathione. Enhanced ROS levels are also detected in neurons under basal conditions, confirming that they are more sensitive to iron variation compared with other cell types. Indeed, we also detected enhanced TfR1 levels in neurons, suggesting iron deficiency. Oxidative damage is commonly associated with iron excess (Arosio and Levi, 2010); however, both in vitro and in vivo evidence suggests, that it can be also induced by iron deficiency. Wan et al. (2012) found that overexpression of wild-type human amyloid-β protein precursor (AβPP) decreased iron levels and increased oxidative stress in neuroblastoma SH-SY5Y cells because of a reduction of catalase activity, suggesting that iron deficiency in AβPP cells may contribute to

the pathogenesis of Alzheimer's disease. Correlation of systemic iron deficiency and serum oxidative stress markers are also reported in patients with anemia (Rajendiran et al., 2012). Our results support the data from previous studies and may be explained by the severe reduction of cytosolic scavenger proteins, such as catalase and SOD1. Catalase and SOD1 proteins may be destabilized, as mRNAs levels are unchanged. Catalase is a heme-containing enzyme and thus iron deprivation limits its functionality (Wan et al., 2012; Kurtoglu et al., 2003). Likewise, apo-catalase is degraded faster. Moreover, the turnover of SOD1 is promoted (Wan et al., 2012; Kurtoglu et al., 2003) by increased H_2O_2 levels as a result of catalase reduction (Pigeolet et al., 1990). Furthermore, ferritin itself is known to be more quickly degraded by cellular iron deprivation (De Domenico et al., 2009). Despite the iron released from damaged ferritin, the LIP remains low. This suggests that the kinetics of iron incorporation into the FtH homopolymer ($K_{m,Fe}$, 80 µM; k_{cat}, 201 min^{-1}; Sun et al., 1993) supersedes the cellular capacity to maintain iron levels. Thus, a FtH homopolymer appears to induce cellular iron deficiency, which is sufficient to affect the antioxidant cellular defense system and to increase ROS levels. ROS trigger the oxidative cascade, inducing accelerated ferritin degradation, which promotes the release of iron from its cavity and contributes to the increase of ROS with the creation of a vicious detrimental cycle. The presence of the two ferritin subunit types thus appears to be crucial to preserve the functionality of the molecule, and the precise H/L subunit ratio is vital to maintaining iron homeostasis.

Iron is essential in several brain processes, such as neurometabolism, myelination, synthesis, and catabolism of neurotransmitters (Rouault and Cooperman, 2006; Snyder and Connor, 2009). Iron deficiency results in impaired brain development, as well as cognitive, behavioral, and psychomotor impairment to name the most worrisome manifestations (Lozoff and Georgieff, 2006). In addition, iron deficiency causes alopecia in mice (Du et al., 2008), whereas in humans a causal link has not been proven (Trost et al., 2006; Daniells and Hardy, 2010). Our patient shows all these phenotypes, supporting the importance of iron availability for brain function and hair loss.

There are conflicting reports as to whether iron deficiency may be involved in the susceptibility to seizures. Mice maintained on an iron deficient diet, with or without addition of lead, showed more spontaneous seizures with a shortened latency of onset compared with those maintained on a normal iron diet (Barzideh et al., 1995), suggesting that iron deficiency improved lead toxicity. A recent epidemiological study on a population with a high prevalence of iron deficiency concluded that there is no association between iron deficiency and acute seizures (Idro et al., 2010). However, the meta-analysis of eight case–control studies that have examined the relationship between iron deficiency and febrile or acute seizures indicated that iron deficiency may be associated with an increased risk of febrile seizures in children (Idro et al., 2010; Sherjil et al., 2010).

Idiopathic generalized epilepsy (IGE) is a group of epilepsy that has very distinct features. It is also called "primary"

generalized epilepsy. Patients with IGE have one or several of three types of (primary generalized) seizures: myoclonic, absence, and generalized tonic-clonic seizures. Up to now, to the best of our knowledge there are no data supporting a higher incidence of IGE in patients with iron deficiency.

On the contrary, the correlation between RLS and iron deficiency is well documented (Connor et al., 2011). RLS is defined as sensorymotor disorder, the key feature of which is an urge to move the legs usually accompanied by abnormal sensations in their legs, particularly during rest (Allen and Earley, 2007). Several clinical and laboratory studies have demonstrated a negative correlation between body iron stores and severity of symptoms (Connor, 2008). Magnetic resonance imaging (MRI) and histochemical studies documented brain iron deficiency in selected brain regions of these patients (Earley et al., 2006; Godau et al., 2008; Snyder et al., 2009). These data stimulated several clinical trials based on iron supplementation in these patients that seems to be efficient in reducing symptoms of RLS (Earley et al., 2009; Cho et al., 2013).

The extended studies in our patient support a causative correlation of diminished cytoplasmic iron availability and the development of epilepsy and RLS. Thus, intracellular iron deficiency, induced by the absence of FtL chain, appears a common cause that may trigger different neurological phenotypes.

MATERIALS AND METHODS

Case. A 23-yr-old female patient was referred to the Department of Hematology of the University Hospital Zürich for further evaluation of iron deficiency. The patient suffered from idiopathic generalized seizures since

the age of 7 yr. A treatment with valproic acid was stopped at the age of 22 yr because of weight gain, progressive hair loss, and no reoccurrence of epilepsy for more than 5 yr. After that, the patient remained without relapse. Both parents of the patient originate from the same region in Calabria and show no relevant medical history; in particular no neurological disorders were present. The patient is not retarded in growth, but shows mild neuropsychological impairment with a reduced intelligence quotient. Therefore, she was not able to finish her pursuit of an assistant nursing job and is receiving disability pension. Due to important progressive hair loss despite the cessation of valproic acid, the general practitioner (GP) performed a check-up. Serum ferritin was below the detection limit (<1 µg/liter) and treatment with 1,400 mg intravenous iron was prescribed by the GP. Interestingly, the ferritin remained unchanged (<1 µg/liter). Beside the remarkable hair loss, physical examination of the patient was unremarkable. Because blood values including hemoglobin concentration, mean corpuscular volume (MCV), mean corpuscular hemoglobin concentration (MCHC), total RBCs, and haptoglobin were normal, we concluded that erythropoiesis was not impaired as a consequence of functional iron deficiency. Furthermore, serum iron levels, transferrin, and transferrin-saturation were within the normal range, implying that systemic iron homeostasis was not affected (Table 2). The reason for the undetectable ferritin was completely unclear. We excluded an antibody-mediated phenomenon by performing a 1:1 mixing test with a normal sample and found no increased reduction of ferritin. Several other commercially available ferritin tests were applied, but the results obtained were equal. To further exclude a transmembrane transport defect, we lysed all blood cells and measured ferritin levels, which were still undetectable. Because of neurological symptoms during childhood and a suspected alteration of ferritin itself, we suggested the diagnosis of a disorder close to neuroferritinopathy even though in this group of patients ferritin is still detectable in serum. However, in repeated MRI no iron deposition in basal ganglia could be found and sequencing of exon 4 of the *FTL1* gene has not identified neuroferritinopathy-associated mutations. An additional neurological examination, including polysomnography, found a restless limb syndrome beside the known idiopathic generalized epilepsy during childhood. To get additional insight into iron deposition, we performed a T2* MRI of

Table 2. Hematological parameters of the patient

Parameter	Value	Reference value
Hemoglobin	140 g/liter	117–153 g/liter
Hematocrit	0.425 liter/liter	0.35–0.46 liter/l
Erythrocytes	4.68 T/liter	3.9–5.2 T/l
MCV	90.8 fl	80–100 fl
MCH	29.9 pg	26–34 pg
MCHC	329 g/liter	310–360 g/liter
Reticulocytes (relative)	1.8%	0.4–2.5%
Reticulocytes (absolute)	83 G/liter	27–132 G/l
Leukocytes	9.15 G/liter	3.0–9.6 G/l
Neutrophils	5.44 G/liter	1.4–8.00 G/l
Monocytes	0.64 G/liter	0.16–0.95 G/l
Eosinophils	0.05 G/liter	0.00–0.70 G/l
Basophils	0.00 G/liter	0.00–0.15 G/l
Lymphocytes	3.02 G/liter	1.50–4.00 G/l
Iron	15.0 µmol/liter	7.0–26.0 µmol/l
Ferritin	< 1.0 µg /liter[a]	10–150 µg /l
Transferrin	28.0 µmol/liter	25–50 µmol/l
Transferrin saturation	27.0%	15–50%
Hepcidin	3.1 nmol/liter	0.5–6.6 nmol/l

Hematological values were determined by clinical methods with the exception of serum hepcidin, which was measured using the Hepcidin 25 bioactive ELISA (DGR International) following the manufacturer's instructions.
[a]Result is outside the reference value.

the liver, which revealed normal iron stores. Because physiologically only FtL can be found in the serum we suspected a previously undescribed mutation in the FtL gene of the patient.

PCR amplification and sequencing of patient DNA. Genomic DNA was extracted from peripheral blood using the QIAamp DNA Blood Mini kit (QIAGEN) according to manufacturer's instructions. PCR amplification of FtL was performed with 70 ng of genomic DNA (for primers see below) with the following conditions: denaturation at 95°C, annealing at 58°C, and extension at 72°C, step 1 and 2 for 30 s, step 3 for 45 s, and for 38 cycles. The resulting amplification products were verified on a 1.5% agarose gel. To remove excess dNTPs and unincorporated primers, 40 µl of PCR product was cleaned by application of the NucleoSpin Gel and PCR Clean-up kit (Machery-Nagel) according to manufacturer's instructions. The purified PCR products were sequenced using the conventional Sanger method by GATC BIOTECH. Sequencing results were analyzed manually using the Chromas software (Technelysium Pty Ltd). F1, 5′-GGGCTGAGACTCCTATGTG-3′; R1, 5′-GACTCCGCCCTCTGTTTACC-3′; F2, 5′-AGCTCCCAG-ATTCGTCAGAA-3′; R2, 5′-CGGTTAAGAGGGCTCACAAG-3′; F3, 5′-GCTACGAGCGTCTCCTGAAG-3′; R3, 5′-CCATCTGGGAGGGA-CAGTTA-3′ (F1+R1→559bp, F2+R2→535bp, F3+R3→1226bp).

Cell culture. We analyzed primary skin fibroblasts from three unaffected subjects (Control: 1, 2 and 3; selected from the Movement Disorders BioBank available at the Neurogenetics Unit of the Neurological Institute "Carlo Besta" (INCB, Milan, Italy) and purchased by ATCC, and our patient who is homozygous for the nucleotide substitution G310T in exon 3 of the FtL gene (E104X). A primary fibroblast cell line was generated from skin biopsy. Fibroblasts were grown in DMEM (Invitrogen) supplemented with 10% FBS (Invitrogen), 100 mg/ml streptomycin, 100 U penicillin, and 2 mM L-glutamine (Sigma-Aldrich).

Fibroblast transduction. 50 multiplicity of infection of VS-pseudotyped lentiviral vector pGK-GFP-Lwt (gift from L. Politi, San Raffaele Scientific Institute, Milan, Italy) was used to transduce 2×10^5 of control (CTR1) and E104X cells. After 48 h, GFP cells were visualized using a fluorescence microscope to test transduction efficiency. The cells were tested for ferritin expression after growth for up to 10 d in DMEM supplemented with 10% FBS, 100 µg/ml streptomycin, 100 U penicillin, and 2 mM L-glutamine; ferritin levels was determined by specific ELISA (Cozzi et al., 1989).

Generation of iNs from human fibroblasts by direct reprogramming. Human fibroblasts from our patient (E104X) and controls (adult fibroblasts from ATCC) were grown in medium for fibroblasts (DMEM, FBS, nonessential amino acids, sodium pyruvate, and penicillin/streptomycin) plated onto Matrigel-coated 24-well plates (5×10^4 cells/well). For immunohistochemical analysis, some of these cells were plated onto Matrigel-coated glass coverslips. The second day, fibroblasts were infected by lentivirus in which cDNAs for transcription factors (Mash1, Nurr1, and Lmx1a) were cloned (Caiazzo et al., 2011) under the control of a tetracycline-responsive promoter. 16–20 h after infection, cells were switched into fresh fibroblast medium containing doxycycline (2 mg/ml) and after further 48 h, the medium was replaced with neuronal inducing medium (DMEM F12, 25 µg/ml insulin, 50 mg/ml transferrin, 30 nM sodium selenite, 20 nM progesterone, and 100 nM putrescine and penicillin/streptomycin) containing doxycycline (all from Sigma). The medium was changed every 2–3 d for further 20 d.

Fluorescence staining. 20 d after viral infection those cells that underwent direct reprogramming were fixed in 4% Paraformaldehyde in PBS for 20 min at room temperature, permeabilized for 30 min in 0,1% Triton X 100, 10% normal goat serum PBS. Then the cells were incubated 1 h at 37°C with mouse anti Beta III tubulin (TuJ1; 1:500; Covance), or with rabbit anti-tyrosine hydroxylase (TH; 1:200; Covance), or with mouse anti-TfR1 (1:1,000; Zymed) antibodies in PBS with 1% BSA. The cells were washed three times with PBS

and incubated for 1 h at 37°C with anti–rabbit or anti–mouse secondary antibody Alexa Fluor 488 or Alexa Fluor 594 (Molecular Probes; 1:500 in PBS, 1% BSA).

RNA extraction and real-time PCR. Total RNA was isolated from fibroblasts cultured in T75 flasks (80% confluence) using the RNeasy kit (QIAGEN) protocol for adherent cells. RNA quantity was measured using a NanoDrop (NanoDrop Technologies), and 1 µg of each sample was incubated with 1 U DNaseI (Invitrogen) for 15 min at room temperature. After DNase inactivation at 65°C for 10 min, RNA was used as a template to generate cDNA by a High-Capacity cDNA Reverse Transcription kit (Applied Biosystems). For negative controls, the reverse transcription was omitted. Reverse transcription products were used in real time PCR to evaluate the expression level of FtL (primers: 5′-ACCTCTCTCTGGGCTTCTAT-3′ and 5′-AGCTGGCTTCTTGATGTCCT-3′), FtH (primers: 5′-CCATGT-CTTACTACTTTGACC-3′ and 5′-GTCTGGTTTCTTGATATCCTG-3′; both synthetized by Primm), catalase (primer: Hs_CAT_1_SG), SOD1 (primer: Hs_SOD1_1_SG; all from QIAGEN) relative to GAPDH with the SYBR Green PCR Master Mix (Applied Biosystems) system.

Cellular ^{55}Fe incorporation. Cells (2×10^5) were incubated for 18 h with 2 µCi/ml ^{55}Fe-ferric ammonium citrate (FAC; Perkin Elmer and Analytical Sciences; ratio 1:2) and 200 µM ascorbic acid (Sigma-Aldrich) in DMEM 0.5% FBS, 0.5% BSA. Cells were washed and lysed in 0.3 ml of lysis buffer (10 mM Hepes, pH 7.4, 137 mM NaCl, 2 mM EDTA, 10% glycerol, and 2% chaps; all from Sigma-Aldrich), and 10 µl of the soluble fraction was mixed with 0.3 ml of Ultima Gold (Packard) and counted for 3 min in a scintillator counter (Packard). 10 µg of soluble fraction was analyzed also on 7% nondenaturing PAGE. Gel was fixed and dried and exposed to autoradiography. The intensity of the ferritin bands was quantified by densitometry.

LIP. Cells (4×10^4) were incubated with 0.250 µM calcein-AM (Invitrogen) for 15 min at 37°C in bicarbonate-free medium containing 1 mg/ml BSA and 20 mM Hepes, pH 7.3. After washing with PBS, HBS (154 mM NaCl and 20 mM Hepes, pH 7.2) was added to the cells, and the fluorescence was monitored at an excitation of 485 nm and an emission of 535 nm on Victor 3 plate reader (Perkin Elmer). The quenching of calcein by intracellular iron was revealed by the addition of 0.2 mM deferiprone.

EMSA. To perform the EMSA, cell extracts (2 µg of total soluble proteins) were incubated with a molar excess of ^{32}P-labeled IRE probe (100,000 cpm) in the presence or absence of 2% β-mercaptoethanol. The IRE probe was generated by in vitro transcription of the plasmid pSPT-fer. The plasmid was linearized with BamHI and transcribed by T7 RNA polymerase in the presence of 80 µCi ^{32}P UTP (ICN; Campanella et al., 2009).

Ferritin quantification and immunoblotting. Ferritin levels were determined by ELISA using the monoclonal antibodies L03 (specific for the FtL) and rH02 (specific for the FtH) calibrated on the corresponding recombinant homopolymer (Cozzi et al., 1989). Protein concentration was evaluated by the bicinchoninic acid (BCA) method (Thermo Fisher Scientific) calibrated on BSA. 20 µg of soluble proteins were separated by sodium dodecyl sulfate–PAGE (SDS-PAGE), and immunoblotting was performed using specific antibodies for Catalase (EMD Millipore), SOD1 (Santa Cruz Biotechnology, Inc.), SOD2 (Santa Cruz Biotechnology, Inc.), TfR1 (Zymed), and β-actin (Sigma-Aldrich), followed by peroxidase-labeled secondary antibodies (Sigma-Aldrich). Band intensity was revealed by enhanced chemiluminescence (ECL; GE Healthcare).

Cell viability assay. 10^4 cells were grown in complete medium for 18 h at 37°C, washed with PBS, incubated for 1 h in serum-free medium, and then added to 0.6 mM H_2O_2 for 2 h. The plates were washed with PBS and cellular viability was measured by incubation with 10 µl MTT solution (5 mg/ml in phosphate-buffered saline) for 2 h at 37°C. Color absorbance was read at 570 nm, following manufacturer's instruction (Sigma-Aldrich; Cozzi et al., 2000).

Reactive oxygen species (ROS) detection. Fibroblasts (10^4) were incubated with 30 µM DHR-123 (Molecular Probes) for 15 min at 37°C, and then washed with PBS and maintained in HBSS supplemented with 1 mM glucose. Fluorescence was determined using the Victor3 Multilabel Counter (PerkinElmer) at 485 and 535 nm for excitation and emission, respectively. Cells were incubated in HBSS for 30 min at 37°C with different amounts of H_2O_2 and, finally, fluorescence was determined as above.

iNs generated from fibroblasts were incubated with Alexa Fluor 647 mouse anti–human CD 56 (N-CAM; BD; dil. 1/40) for 1 h, with 20 µM $2',7'$-DCF (CM-H_2CFDA; Molecular Probes) for 15 min, and with 2 µg/ml of Hoechst 33342 for 3 min. All of these incubations were performed at 37°C. Cells were washed and analyzed by IN-Cell Analyzer 1000 system (GE Healthcare). Fluorescence of DCF from N-CAM–positive cells was collected to compare the relative ROS content.

Mitochondrial membrane potential assay. The same fluorescent detection procedure described above was performed to determine mitochondrial membrane potential using Alexa Fluor 488 mouse anti–human N-CAM (BD; dil.1/40) and 20 nM TMRM treatment for 15 min.

Glutathione assay. 10^4 cells were plated in complete medium and treated with 5 mM of TCEP (tris[2-carboxyethyl]phosphine) for 20 min at room temperature. GSH-Glo Reagent and Luciferin Detection Reagent, according to Promega protocol kit, were added and the plates were incubated at room temperature for 30 and 15 min, respectively. Finally, the luminescence was read on Victor 3 reader (Perkin Elmer).

Oxidized protein detection. Oxidized proteins were detected using the Oxyblot Protein Oxidation Detection kit (EMD Millipore) following manufacturer's instructions. In brief, the soluble protein extracts were derivatized to 2,4-dinitrophenylhydrazone (DNP), and 1 µg was loaded on 12% SDS-PAGE, blotted, and incubated with an anti-DNP antibody. The bound activity was revealed by ECL advance (GE Healthcare).

SOD activity measurement. Total cell homogenates (15 µg) were analyzed for SOD activity after separation on a 12% nondenaturing PAGE with nitro blue tetrazolium staining (White et al., 1993). In brief, the gels were stained with 0.025% nitro blue tetrazolium (Sigma-Aldrich) and 0.01% riboflavin (Sigma-Aldrich) dissolved in H_2O for 20 min in the dark. 1% N,N,N′,N′-Tetramethylethylene-diamine (Temed; Sigma-Aldrich) was then added to the solution, and the gel was exposed to light for 10 min. Finally, the gel was washed with H_2O.

Metabolic labeling and immunoprecipitation. Cells were metabolically labeled, as previously described (Cozzi et al., 2004). In brief, 5×10^5 cells were grown for 1 h in DMEM without L-glutamine, methionine, and cysteine (ICN), 0.5% BSA, 0.5% FBS, and then 50 µCi/ml [^{35}S]methionine and [^{35}S]cysteine (ICN) was added and the cells were grown for other 18 h. The cells were suspended with lysis buffer (20 mM Tris-HCl, pH 8.0, 200 mM LiCl, 1 mM EDTA, and 0.5% Nonidet P-40), and the total radioactivity of the soluble proteins was determined by trichloroacetic acid precipitation. Cytosolic lysates (4×10^6 cpm) were immunoprecipitated (Cozzi et al., 2000) by adding anti–FtL antibody, and then the soluble fraction was precipitated again with an anti–FtH antibody and analyzed on 12% SDS-PAGE. The gels were treated with autoradiography image enhancer (Amplify), dried, and exposed to autoradiography. For evaluation of ferritin degradation, the cells were labeled with [^{35}S]methionine, [^{35}S]cysteine for 18 h, and then washed twice with PBS and grown in the complete medium. The cells were harvested and lysed at the times indicates, and 10 µg of soluble extract protein was subjected to immunoprecipitation with anti–FtH antibody as above. The intensity of ferritin subunit bands was quantified by densitometry.

Statistical analyses. The data, except where otherwise indicated, are reported as the mean ± SD values or as a representative of at least three independent experiments with similar results. Statistically significant differences between controls and patients were determined by the Student's *t* test, which was considered significant when $P \leq 0.05$.

REFERENCES

Allen, R. 2004. Dopamine and iron in the pathophysiology of restless legs syndrome (RLS). *Sleep Med.* 5:385–391. http://dx.doi.org/10.1016/j.sleep.2004.01.012

Allen, R.P., and C.J. Earley. 2007. The role of iron in restless legs syndrome. *Mov. Disord.* 22(Suppl 18):S440–S448. http://dx.doi.org/10.1002/mds.21607

Allen, R.P., P.B. Barker, F. Wehrl, H.K. Song, and C.J. Earley. 2001. MRI measurement of brain iron in patients with restless legs syndrome. *Neurology.* 56:263–265. http://dx.doi.org/10.1212/WNL.56.2.263

Altamura, S., and M.U. Muckenthaler. 2009. Iron toxicity in diseases of aging: Alzheimer's disease, Parkinson's disease and atherosclerosis. *J. Alzheimers Dis.* 16:879–895.

Arosio, P., and S. Levi. 2010. Cytosolic and mitochondrial ferritins in the regulation of cellular iron homeostasis and oxidative damage. *Biochim. Biophys. Acta.* 1800:783–792. http://dx.doi.org/10.1016/j.bbagen.2010.02.005

Barzideh, O., R.G. Burright, and P.J. Donovick. 1995. Dietary iron and exposure to lead influence susceptibility to seizures. *Psychol. Rep.* 76:971–976. http://dx.doi.org/10.2466/pr0.1995.76.3.971

Beaumont, C., P. Leneuve, I. Devaux, J.Y. Scoazec, M. Berthier, M.N. Loiseau, B. Grandchamp, and D. Bonneau. 1995. Mutation in the iron responsive element of the L ferritin mRNA in a family with dominant hyperferritinaemia and cataract. *Nat. Genet.* 11:444–446. http://dx.doi.org/10.1038/ng1295-444

Berg, D., and M.B. Youdim. 2006. Role of iron in neurodegenerative disorders. *Top. Magn. Reson. Imaging.* 17:5–17. http://dx.doi.org/10.1097/01.rmr.0000245461.90406.ad

Brooks, D.G., K. Manova-Todorova, J. Farmer, L. Lobmayr, R.B. Wilson, R.C. Eagle Jr., T.G. St Pierre, and D. Stambolian. 2002. Ferritin crystal cataracts in hereditary hyperferritinemia cataract syndrome. *Invest. Ophthalmol. Vis. Sci.* 43:1121–1126.

Burn, J., and P.F. Chinnery. 2006. Neuroferritinopathy. *Semin. Pediatr. Neurol.* 13:176–181. http://dx.doi.org/10.1016/j.spen.2006.08.006

Caiazzo, M., M.T. Dell'Anno, E. Dvoretskova, D. Lazarevic, S. Taverna, D. Leo, T.D. Sotnikova, A. Menegon, P. Roncaglia, G. Colciago, et al. 2011. Direct generation of functional dopaminergic neurons from mouse and human fibroblasts. *Nature.* 476:224–227. http://dx.doi.org/10.1038/nature10284

Campanella, A., E. Rovelli, P. Santambrogio, A. Cozzi, F. Taroni, and S. Levi. 2009. Mitochondrial ferritin limits oxidative damage regulating mitochondrial iron availability: hypothesis for a protective role in Friedreich ataxia. *Hum. Mol. Genet.* 18:1–11. http://dx.doi.org/10.1093/hmg/ddn308

Cho, Y.W., R.P. Allen, and C.J. Earley. 2013. Lower molecular weight intravenous iron dextran for restless legs syndrome. *Sleep Med.* 14:274–277. http://dx.doi.org/10.1016/j.sleep.2012.11.001

Clardy, S.L., X. Wang, W. Zhao, W. Liu, G.A. Chase, J.L. Beard, B. True Felt, and J.R. Connor. 2006. Acute and chronic effects of developmental iron deficiency on mRNA expression patterns in the brain. *J. Neural Transm. Suppl.* 71:173–196. http://dx.doi.org/10.1007/978-3-211-33328-0_19

Connor, J.R. 2008. Pathophysiology of restless legs syndrome: evidence for iron involvement. *Curr. Neurol. Neurosci. Rep.* 8:162–166. http://dx.doi.org/10.1007/s11910-008-0026-x

Connor, J.R., P. Ponnuru, X.S. Wang, S.M. Patton, R.P. Allen, and C.J. Earley. 2011. Profile of altered brain iron acquisition in restless legs syndrome. *Brain*. 134:959–968. http://dx.doi.org/10.1093/brain/awr012

Cozzi, A., S. Levi, E. Bazzigaluppi, G. Ruggeri, and P. Arosio. 1989. Development of an immunoassay for all human isoferritins, and its application to serum ferritin evaluation. *Clin. Chim. Acta*. 184:197–206. http://dx.doi.org/10.1016/0009-8981(89)90052-1

Cozzi, A., B. Corsi, S. Levi, P. Santambrogio, A. Albertini, and P. Arosio. 2000. Overexpression of wild type and mutated human ferritin H–chain in HeLa cells: in vivo role of ferritin ferroxidase activity. *J. Biol. Chem*. 275:25122–25129. http://dx.doi.org/10.1074/jbc.M003797200

Cozzi, A., B. Corsi, S. Levi, P. Santambrogio, G. Biasiotto, and P. Arosio. 2004. Analysis of the biologic functions of H- and L-ferritins in HeLa cells by transfection with siRNAs and cDNAs: evidence for a proliferative role of L-ferritin. *Blood*. 103:2377–2383. http://dx.doi.org/10.1182/blood-2003-06-1842

Cozzi, A., P. Santambrogio, B. Corsi, A. Campanella, P. Arosio, and S. Levi. 2006. Characterization of the l-ferritin variant 460InsA responsible of a hereditary ferritinopathy disorder. *Neurobiol. Dis*. 23:644–652. http://dx.doi.org/10.1016/j.nbd.2006.05.004

Cozzi, A., E. Rovelli, G. Frizzale, A. Campanella, M. Amendola, P. Arosio, and S. Levi. 2010. Oxidative stress and cell death in cells expressing L-ferritin variants causing neuroferritinopathy. *Neurobiol. Dis*. 37:77–85. http://dx.doi.org/10.1016/j.nbd.2009.09.009

Cremonesi, L., A. Cozzi, D. Girelli, F. Ferrari, I. Fermo, B. Foglieni, S. Levi, C. Bozzini, M. Camparini, M. Ferrari, and P. Arosio. 2004. Case report: a subject with a mutation in the ATG start codon of L–ferritin has no haematological or neurological symptoms. *J. Med. Genet*. 41:e81. http://dx.doi.org/10.1136/jmg.2003.011718

Curtis, A.R., C. Fey, C.M. Morris, L.A. Bindoff, P.G. Ince, P.F. Chinnery, A. Coulthard, M.J. Jackson, A.P. Jackson, D.P. McHale, et al. 2001. Mutation in the gene encoding ferritin light polypeptide causes dominant adult-onset basal ganglia disease. *Nat. Genet*. 28:350–354. http://dx.doi.org/10.1038/ng571

Daniells, S., and G. Hardy. 2010. Hair loss in long-term or home parenteral nutrition: are micronutrient deficiencies to blame? *Curr. Opin. Clin. Nutr. Metab. Care*. 13:690–697. http://dx.doi.org/10.1097/MCO.0b013e32833ece02

Darshan, D., L. Vanoaica, L. Richman, F. Beermann, and L.C. Kühn. 2009. Conditional deletion of ferritin H in mice induces loss of iron storage and liver damage. *Hepatology*. 50:852–860. http://dx.doi.org/10.1002/hep.23058

De Domenico, I., D.M. Ward, and J. Kaplan. 2009. Specific iron chelators determine the route of ferritin degradation. *Blood*. 114:4546–4551. http://dx.doi.org/10.1182/blood-2009-05-224188

Du, X., E. She, T. Gelbart, J. Truksa, P. Lee, Y. Xia, K. Khovananth, S. Mudd, N. Mann, E.M. Moresco, et al. 2008. The serine protease TMPRSS6 is required to sense iron deficiency. *Science*. 320:1088–1092. http://dx.doi.org/10.1126/science.1157121

Earley, C.J., P B Barker, A. Horská, and R.P. Allen. 2006. MRI–determined regional brain iron concentrations in early- and late-onset restless legs syndrome. *Sleep Med*. 7:458–461. http://dx.doi.org/10.1016/j.sleep.2005.11.009

Earley, C.J., A. Horská, M.A. Mohamed, P.B. Barker, J.L. Beard, and R.P. Allen. 2009. A randomized, double-blind, placebo-controlled trial of intravenous iron sucrose in restless legs syndrome. *Sleep Med*. 10:206–211. http://dx.doi.org/10.1016/j.sleep.2007.12.006

Ferreira, C., D. Bucchini, M.E. Martin, S. Levi, P. Arosio, B. Grandchamp, and C. Beaumont. 2000. Early embryonic lethality of H ferritin gene deletion in mice. *J. Biol. Chem*. 275:3021–3024. http://dx.doi.org/10.1074/jbc.275.5.3021

Ferreira, C., P. Santambrogio, M.E. Martin, V. Andrieu, G. Feldmann, D. Hénin, and C. Beaumont. 2001. H ferritin knockout mice: a model of hyperferritinemia in the absence of iron overload. *Blood*. 98:525–532. http://dx.doi.org/10.1182/blood.V98.3.525

Ford, G.C., P.M. Harrison, D.W. Rice, J.M. Smith, A. Treffry, J.L. White, and J. Yariv. 1984. Ferritin: design and formation of an iron-storage molecule. *Philos. Trans. R. Soc. Lond. B Biol. Sci*. 304:551–565. http://dx.doi.org/10.1098/rstb.1984.0046

Godau, J., U. Klose, A. Di Santo, K. Schweitzer, and D. Berg. 2008. Multiregional brain iron deficiency in restless legs syndrome. *Mov. Disord*. 23:1184–1187. http://dx.doi.org/10.1002/mds.22070

Hayflick, S.J. 2006. Neurodegeneration with brain iron accumulation: from genes to pathogenesis. *Semin. Pediatr. Neurol*. 13:182–185. http://dx.doi.org/10.1016/j.spen.2006.08.007

Hentze, M.W., M.U. Muckenthaler, B. Galy, and C. Camaschella. 2010. Two to tango: regulation of Mammalian iron metabolism. *Cell*. 142:24–38. http://dx.doi.org/10.1016/j.cell.2010.06.028

Idro, R., S. Gwer, T.N. Williams, T. Otieno, S. Uyoga, G. Fegan, P.A. Kager, K. Maitland, F. Kirkham, B.G. Neville, and C.R. Newton. 2010. Iron deficiency and acute seizures: results from children living in rural Kenya and a meta-analysis. *PLoS ONE*. 5:e14001. http://dx.doi.org/10.1371/journal.pone.0014001

Isken, O., and L.E. Maquat. 2007. Quality control of eukaryotic mRNA: safeguarding cells from abnormal mRNA function. *Genes Dev*. 21:1833–1856. http://dx.doi.org/10.1101/gad.1566807

Jeong, S.Y., D.R. Crooks, H. Wilson-Ollivierre, M.C. Ghosh, R. Sougrat, J. Lee, S. Cooperman, J.B. Mitchell, C. Beaumont, and T.A. Rouault. 2011. Iron insufficiency compromises motor neurons and their mitochondrial function in Irp2-null mice. *PLoS ONE*. 6:e25404. http://dx.doi.org/10.1371/journal.pone.0025404

Kannengiesser, C., A.M. Jouanolle, G. Hetet, A. Mosser, F. Muzeau, D. Henry, E. Bardou-Jacquet, M. Mornet, P. Brissot, Y. Deugnier, et al. 2009. A new missense mutation in the L ferritin coding sequence associated with elevated levels of glycosylated ferritin in serum and absence of iron overload. *Haematologica*. 94:335–339. http://dx.doi.org/10.3324/haematol.2008.000125

Kurtoglu, E., A. Ugur, A.K. Baltaci, and L. Undar. 2003. Effect of iron supplementation on oxidative stress and antioxidant status in iron-deficiency anemia. *Biol. Trace Elem. Res*. 96:117–123. http://dx.doi.org/10.1385/BTER:96:1-3:117

Langlois d'Estaintot, B., P. Santambrogio, T. Granier, B. Gallois, J.M. Chevalier, G. Précigoux, S. Levi, and P. Arosio. 2004. Crystal structure and biochemical properties of the human mitochondrial ferritin and its mutant Ser144Ala. *J. Mol. Biol*. 340:277–293. http://dx.doi.org/10.1016/j.jmb.2004.04.036

Lawson, D.M., P.J. Artymiuk, S.J. Yewdall, J.M. Smith, J.C. Livingstone, A. Treffry, A. Luzzago, S. Levi, P. Arosio, G. Cesareni, et al. 1991. Solving the structure of human H ferritin by genetically engineering intermolecular crystal contacts. *Nature*. 349:541–544. http://dx.doi.org/10.1038/349541a0

Levi, S., and P. Arosio. 2004. Mitochondrial ferritin. *Int. J. Biochem. Cell Biol*. 36:1887–1889. http://dx.doi.org/10.1016/j.biocel.2003.10.020

Levi, S., A. Luzzago, G. Cesareni, A. Cozzi, F. Franceschinelli, A. Albertini, and P. Arosio. 1988. Mechanism of ferritin iron uptake: activity of the H-chain and deletion mapping of the ferro-oxidase site. A study of iron uptake and ferro-oxidase activity of human liver, recombinant H-chain ferritins, and of two H-chain deletion mutants. *J. Biol. Chem*. 263:18086–18092.

Levi, S., A. Luzzago, F. Franceschinelli, P. Santambrogio, G. Cesareni, and P. Arosio. 1989. Mutational analysis of the channel and loop sequences of human ferritin H–chain. *Biochem. J*. 264:381–388.

Levi, S., S.J. Yewdall, P.M. Harrison, P. Santambrogio, A. Cozzi, E. Rovida, A. Albertini, and P. Arosio. 1992. Evidence of H- and L-chains have co-operative roles in the iron-uptake mechanism of human ferritin. *Biochem. J*. 288:591–596.

Levi, S., P. Santambrogio, A. Cozzi, E. Rovida, B. Corsi, E. Tamborini, S. Spada, A. Albertini, and P. Arosio. 1994. The role of the L-chain in ferritin iron incorporation. Studies of homo and heteropolymers. *J. Mol. Biol*. 238:649–654. http://dx.doi.org/10.1006/jmbi.1994.1325

Levi, S., B. Corsi, M. Bosisio, R. Invernizzi, A. Volz, D. Sanford, P. Arosio, and J. Drysdale. 2001. A human mitochondrial ferritin encoded by an intron-less gene. *J. Biol. Chem*. 276:24437–24440. http://dx.doi.org/10.1074/jbc.C100141200

Levi, S., A. Cozzi, and P. Arosio. 2005. Neuroferritinopathy: a neurodegenerative disorder associated with L-ferritin mutation. *Best Pract. Res. Clin. Haematol*. 18:265–276. http://dx.doi.org/10.1016/j.beha.2004.08.021

Absence of FtL causes neurological symptoms. | Cozzi et al.

Lozoff, B., and M.K. Georgieff. 2006. Iron deficiency and brain development. *Semin. Pediatr. Neurol.* 13:158–165. http://dx.doi.org/10.1016/j.spen .2006.08.004

Luscieti, S., P. Santambrogio, B. Langlois d'Estaintot, T. Granier, A. Cozzi, M. Poli, B. Gallois, D. Finazzi, A. Cattaneo, S. Levi, and P. Arosio. 2010. Mutant ferritin L-chains that cause neurodegeneration act in a domi-nant-negative manner to reduce ferritin iron incorporation. *J. Biol. Chem.* 285:11948–11957. http://dx.doi.org/10.1074/jbc.M109.096404

Mehlhase, J., G. Sandig, K. Pantopoulos, and T. Grune. 2005. Oxidation-induced ferritin turnover in microglial cells: role of proteasome. *Free Radic. Biol. Med.* 38:276–285. http://dx.doi.org/10.1016/j.freeradbiomed.2004 .10.025

Millonig, G., M.U. Muckenthaler, and S. Mueller. 2010. Hyperferritinaemia-cataract syndrome: worldwide mutations and phenotype of an increas-ingly diagnosed genetic disorder. *Hum. Genomics.* 4:250–262.

Missirlis, F., S. Kosmidis, T. Brody, M. Mavrakis, S. Holmberg, W.F. Odenwald, E.M. Skoulakis, and T.A. Rouault. 2007. Homeostatic mechanisms for iron storage revealed by genetic manipulations and live imag-ing of Drosophila ferritin. *Genetics.* 177:89–100. http://dx.doi.org/10 .1534/genetics.107.075150

Ozaydin, E., E. Arhan, B. Cetinkaya, S. Ozdel, A. Değerliyurt, A. Güven, and G. Köse. 2012. Differences in iron deficiency anemia and mean plate-let volume between children with simple and complex febrile seizures. *Seizure.* 21:211–214. http://dx.doi.org/10.1016/j.seizure.2011.12.014

Picard, V., S. Epsztejn, P. Santambrogio, Z.I. Cabantchik, and C. Beaumont. 1998. Role of ferritin in the control of the labile iron pool in murine erythroleukemia cells. *J. Biol. Chem.* 273:15382–15386. http://dx.doi .org/10.1074/jbc.273.25.15382

Pigeolet, E., P. Corbisier, A. Houbion, D. Lambert, C. Michiels, M. Raes, M.D. Zachary, and J. Remacle. 1990. Glutathione peroxidase, super-oxide dismutase, and catalase inactivation by peroxides and oxygen derived free radicals. *Mech. Ageing Dev.* 51:283–297. http://dx.doi .org/10.1016/0047-6374(90)90078-T

Rajendiran, S., B. Zachariah, and A. Hamide. 2012. Increased protein car-bonylation and decreased antioxidant status in anemic H. pylori infected patients: effect of treatment. *Saudi J. Gastroenterol.* 18:252–256. http:// dx.doi.org/10.4103/1319-3767.98430

Recalcati, S., G. Minotti, and G. Cairo. 2010. Iron regulatory proteins: from molecular mechanisms to drug development. *Antioxid. Redox Signal.* 13:1593–1616. http://dx.doi.org/10.1089/ars.2009.2983

Romão, L., A. Inácio, S. Santos, M. Avila, P. Faustino, P. Pacheco, and J. Lavinha. 2000. Nonsense mutations in the human beta-globin gene lead to unexpected levels of cytoplasmic mRNA accumulation. *Blood.* 96:2895–2901.

Rouault, T.A., and S. Cooperman. 2006. Brain iron metabolism. *Semin. Pediatr. Neurol.* 13:142–148. http://dx.doi.org/10.1016/j.spen.2006.08.002

Salas, R.E., C.E. Gamaldo, and R.P. Allen. 2010. Update in restless legs syndrome. *Curr. Opin. Neurol.* 23:401–406.

Santambrogio, P., S. Levi, P. Arosio, L. Palagi, G. Vecchio, D.M. Lawson, S.J. Yewdall, P.J. Artymiuk, P.M. Harrison, R. Jappelli, et al. 1992. Evidence that a salt bridge in the light chain contributes to the physi-cal stability difference between heavy and light human ferritins. *J. Biol. Chem.* 267:14077–14083.

Santambrogio, P., S. Levi, A. Cozzi, E. Rovida, A. Albertini, and P. Arosio. 1993. Production and characterization of recombinant heteropolymers of human ferritin H and L chains. *J. Biol. Chem.* 268:12744–12748.

Schulz, J.B., J. Lindenau, J. Seyfried, and J. Dichgans. 2000. Glutathione, oxidative stress and neurodegeneration. *Eur. J. Biochem.* 267:4904–4911. http://dx.doi.org/10.1046/j.1432-1327.2000.01595.x

Sherjil, A., Z. us Saeed, S. Shehzad, and R. Amjad. 2010. Iron deficiency anaemia—a risk factor for febrile seizures in children. *J. Ayub Med. Coll. Abbottabad.* 22:71–73.

Snyder, A.M., and J.R. Connor. 2009. Iron, the substantia nigra and related neurological disorders. *Biochim. Biophys. Acta.* 1790:606–614. http:// dx.doi.org/10.1016/j.bbagen.2008.08.005

Snyder, A.M., X. Wang, S.M. Patton, P. Arosio, S. Levi, C.J. Earley, R.P. Allen, and J.R. Connor. 2009. Mitochondrial ferritin in the substantia nigra in restless legs syndrome. *J. Neuropathol. Exp. Neurol.* 68:1193–1199. http:// dx.doi.org/10.1097/NEN.0b013e3181bdc44f

Sun, S., P. Arosio, S. Levi, and N.D. Chasteen. 1993. Ferroxidase kinetics of human liver apoferritin, recombinant H-chain apoferritin, and site-directed mutants. *Biochemistry.* 32:9362–9369. http://dx.doi.org/10.1021/ bi00087a015

Thompson, K., S. Menzies, M. Muckenthaler, F.M. Torti, T. Wood, S.V. Torti, M.W. Hentze, J. Beard, and J. Connor. 2003. Mouse brains deficient in H-ferritin have normal iron concentration but a protein profile of iron deficiency and increased evidence of oxidative stress. *J. Neurosci. Res.* 71:46–63. http://dx.doi.org/10.1002/jnr.10463

Thurlow, V., B. Vadher, A. Bomford, C. DeLord, C. Kannengiesser, C. Beaumont, and B. Grandchamp. 2012. Two novel mutations in the L fer-ritin coding sequence associated with benign hyperferritinaemia un-masked by glycosylated ferritin assay. *Ann. Clin. Biochem.* 49:302–305. http://dx.doi.org/10.1258/acb.2011.011229

Trost, L.B., W.F. Bergfeld, and E. Calogeras. 2006. The diagnosis and treat-ment of iron deficiency and its potential relationship to hair loss. *J. Am. Acad. Dermatol.* 54:824–844. http://dx.doi.org/10.1016/j.jaad.2005.11 .1104

Vidal, R., B. Ghetti, M. Takao, C. Brefel-Courbon, E. Uro-Coste, B.S. Glazier, V. Siani, M.D. Benson, P. Calvas, L. Miravalle, et al. 2004. Intracellular ferritin accumulation in neural and extraneural tissue characterizes a neurodegenerative disease associated with a mutation in the ferritin light polypeptide gene. *J. Neuropathol. Exp. Neurol.* 63: 363–380.

Vierbuchen, T., and M. Wernig. 2011. Direct lineage conversions: unnatu-ral but useful? *Nat. Biotechnol.* 29:892–907. http://dx.doi.org/10.1038/ nbt.1946

Wan, L., G. Nie, J. Zhang, and B. Zhao. 2012. Overexpression of human wild-type amyloid-β protein precursor decreases the iron content and increases the oxidative stress of neuroblastoma SH-SY5Y cells. *J. Alzheimers Dis.* 30:523–530.

White, C.W., D.H. Nguyen, K. Suzuki, N. Taniguchi, L.S. Rusakow, K.B. Avraham, and Y. Groner. 1993. Expression of manganese superoxide dis-mutase is not altered in transgenic mice with elevated level of copper-zinc superoxide dismutase. *Free Radic. Biol. Med.* 15:629–636. http://dx.doi .org/10.1016/0891-5849(93)90166-R

Yewdall, S.J., D.M. Lawson, P.J. Artymiuk, A. Treffry, P.M. Harrison, A. Luzzago, G. Cesareni, S. Levi, and P. Arosio. 1990. Structural studies on recombinant human ferritins. *Biochem. Soc. Trans.* 18:1028–1029.

Zhao, G., F. Bou-Abdallah, P. Arosio, S. Levi, C. Janus-Chandler, and N.D. Chasteen. 2003. Multiple pathways for mineral core formation in mam-malian apoferritin. The role of hydrogen peroxide. *Biochemistry.* 42:3142– 3150. http://dx.doi.org/10.1021/bi027357v